Published in Journal of Hydrology 193, issue 1-4, 306-315, 1997
which should be used for any reference to this work

Numerical simulation as a tool for checking the interpretation of karst spring hydrographs

Laurent Eisenlohr[a,*], László Király[a], Mahmoud Bouzelboudjen[a], Yvan Rossier[b]

[a]*University of Neuchâtel, Centre of Hydrogeology, 11 Emile-Argand, 2007 Neuchâtel, Switzerland*
[b]*Ministry of Environment, Department of Water and Aquatic Media, 1 Verdun, 21067 Dijon, France*

Abstract

A schematic representation of karst aquifers may be that of a high hydraulic conductivity channel network with kilometre-wide intervals, surrounded by a low hydraulic conductivity fractured limestone volume and connected to a local discharge area, the karst spring. The behaviour of the karst spring (hydrographs, chemical or isotopic composition, etc.) represents the global response of the karst aquifer to input events.

The available data on karst aquifer hydraulic parameters are limited. Global response is therefore more easily obtained and is commonly used to make inferences on the recharge and groundwater flow processes, as well as on the hydraulic parameter fields. Direct verification of these interpretations is, obviously, very difficult.

We have used an indirect method of verification, consisting of introducing well-defined theoretical karst structures into a finite element model and then analysing the simulated global response according to presently accepted interpretation schemes. As we know what we put into the numerical model, the validity of any interpretation may be checked.

The first results indicate that some of the generally accepted interpretations are not necessarily true. In particular: (i) separation of simulated recession hydrographs into several components shows that different exponential components do not necessarily correspond to aquifer volumes with different hydraulic conductivities; (ii) non-exponential parts of recession hydrographs do not always give information about the infiltration process; and (iii) the recession coefficient of the baseflow (i.e. the last, nearly exponential part of the recession hydrograph) depends on the global configuration of the whole karst aquifer, not just on the hydraulic properties of the low hydraulic conductivity volumes.

* Corresponding author present address: GHT 130, Gästehaus der Uni. Bremen, 58 Teerhof, 28199 Bremen, Germany.

1. Introduction

In karst aquifers, besides the low hydraulic conductivity common fracture network with spacings of a few metres, there is a high hydraulic conductivity channel network with kilometre-wide intervals, which is well connected to a small and narrow discharge area, the karst spring. According to Király et al. (1995), the duality of karst aquifers is a direct consequence of this structure (see Fig. 1A and 1B): (1) duality of the infiltration processes (diffuse or slow infiltration into the low hydraulic conductivity volume, concentrated or rapid infiltration into the channel network); (2) duality of the groundwater flow field (low flow velocities in the fractured volume, high flow velocities in the channel network); and (3) duality of the discharge conditions (diffuse seepage from the low hydraulic conductivity volume, concentrated discharge from the channel network, at the karst spring).

The typical behaviour of the karst spring, i.e. rapid variation of the spring discharge, rapid variation of the chemical and isotopic composition of the spring water, etc., represents the global response of the heterogeneous karst aquifer to input events (Schoeller, 1967; Király, 1975; Atkinson, 1977). Available data on the three-dimensional distribution of the hydraulic heads and hydraulic parameters are very limited. Therefore, the more

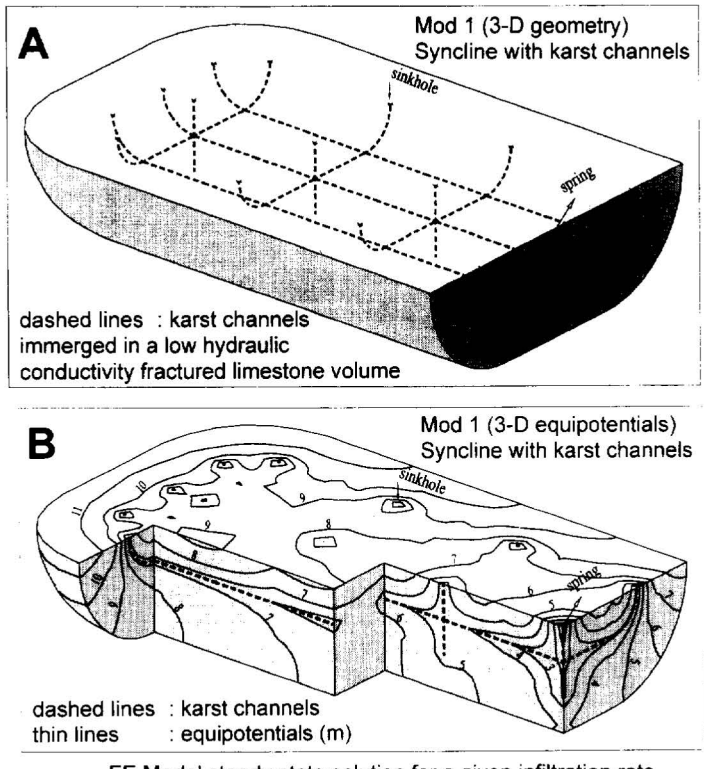

Fig. 1. A: Theoretical karst syncline simulated by quadratic finite element model. B: Field of the hydraulic potentials (after Király et al., 1995).

easily obtained global response is often used to make inferences on the infiltration and groundwater flow processes, as well as on the hydraulic parameter fields.

In most cases, interpretations are based on the analysis of recession hydrographs by using the different hydrograph separation methods (Forkasiewicz and Paloc, 1967; Drogue, 1972; Mangin, 1975; Soulios, 1991; Padilla et al., 1994; Bonacci, 1987, Bonacci, 1993), statistical analysis of the whole spring hydrograph (Mangin, 1984; Dreiss, 1982), or analysis of transfer functions between input (infiltration) and output (spring hydrograph) obtained by black-box or grey-box models. All these methods will be referred to as global methods, because they use the global response of the karst aquifer to input events.

Direct verification of interpretations based on global methods is obviously very difficult because of the scarcity of empirical observations in real karst aquifers. An indirect method of verification would be to introduce well-defined, theoretical karst structures into a deterministic numerical model and then analyse the simulated global response (i.e. the simulated spring hydrograph) according to the global methods presently used. As the user knows exactly what is put into the deterministic flow model, the plausibility of the interpretations obtained by the global methods can be quickly checked, at least to some extent. This is the problem that we address in the present paper.

2. Interpretation of karst spring hydrographs based on the global methods

Spring discharge and chemistry of spring water are the most easily measurable parameters which characterize the global behaviour of karst aquifers. This section presents a few methods that are widely used to describe and analyse karst spring hydrographs.

2.1. Analysis of recession hydrographs

The recession curve is that part of the spring flow hydrograph which extends from a peak to the start of the next rise. Several mathematical functions have been used to describe the recession hydrograph, with or without physical interpretation. In one of the most popular methods, Forkasiewicz and Paloc (1967) proposed that the total recession curve be represented as the sum of two, three or more exponential functions:

$$Q(t) = \sum_{i=1}^{N} Q_{0_i} e^{-\alpha_i t} \tag{1}$$

where N is the number of exponentials, t is the time, Q_{0_i} are the discharges at $t = 0$ and α_i are the recession coefficients for each exponential. In the interpretation, each exponential is thought to represent the depletion of a reservoir, the hydraulic conductivity of the reservoir being proportional to the recession coefficients α_i. According to this interpretation, the exponential with the highest recession coefficient α_N would represent the rapid depletion of the karst channels with high hydraulic conductivity and the exponential with the lowest recession coefficient α_1 would correspond to the baseflow, i.e. to the slow depletion of the low hydraulic conductivity fracture network. Intermediate exponentials are thought to represent the emptying of aquifer volumes with intermediate values of hydraulic conductivity. As shown by Király and Morel (1976), the interpretation of the intermediate exponentials is not necessarily true.

Another, widely used, method was proposed by Mangin (1975). In this method, the total recession curve is separated into an exponential component, interpreted as the baseflow, and a non-exponential component, which would represent the effect of rapid infiltrations from the surface (Padilla et al., 1994). The recession is described by the formula

$$Q(t) = (Q_0 - Q_{R0})\frac{(1-\eta t)}{(1+\varepsilon t)} + Q_{R0}e^{-\alpha t} \tag{2}$$

where t is the time, Q_0 and Q_{R0} are the total spring discharge and the baseflow at $t = 0$, α is the recession coefficient for the baseflow, and the difference $(Q_0 - Q_{R0}) = q_0$ represents the amount of the rapid infiltrations at $t = 0$. The parameters ε and η are determined empirically to fit the non-exponential part of the recession curve and play a very important role in the interpretation scheme of Mangin. It is assumed, for example, that the time interval between $t = 0$ and $t = 1/\eta$ represents the duration of the infiltration, ε being a coefficient of heterogeneity. In other words, there is no more infiltration for $t > 1/\eta$ and the first term on the right-hand side of Eq. (2) is zero.

2.2. Analysis of the spring hydrograph by autocorrelation

In this method, we analyse the entire spring flow hydrograph and the corresponding precipitation for periods extending from a few months to several years. The hydrograph is transformed into a discretized time series of N terms $(x_1 \ldots x_i \ldots x_N)$ for which we calculate m autocorrelation coefficients $(r_0 \ldots r_k \ldots r_m)$. Recommended values are $m = N/3$ (Mangin, 1984) or $m = N/2$ (Box and Jenkins, 1974), but other values may be used, for example $m = 2N/3$. The autocorrelation coefficients are given by

$$r_k = \frac{C_k}{C_0} \tag{3}$$

with

$$C_0 = \frac{1}{N}\sum_{i=1}^{N}(x_i - \bar{x})^2 \tag{4}$$

and

$$C_k = \frac{1}{N}\sum_{i=1}^{N\pm k}(x_i - \bar{x})(x_{i+k} - \bar{x}) \tag{5}$$

where $\bar{x}$ is the arithmetic mean of the x_i values and $k = 0,\ldots,m$. The graph of the r_k values is a simple correlogram and its shape is supposed to give information about the memory effect, the karstification, and the groundwater reserves of the karst aquifer (e.g. Mangin, 1984).

The cross-correlation between rainfall and spring discharge is the impulse response of the karst system, giving information about the quality of drainage and the groundwater reserves of the aquifer (Mangin, 1984).

3. Numerical simulation of the groundwater flow in karst aquifers

As pointed out in the Introduction, karst aquifers may be represented by a high hydraulic

conductivity, kilometre-wide channel network connected to the karst spring and surrounded by a low hydraulic conductivity, fractured limestone volume. Finite element numerical models are particularly well suited to simulate groundwater flow in such heterogeneous media, provided they allow for the combination of 1-D, 2-D and 3-D finite elements, as proposed by Király (1979, 1985, 1988) and Király et al. (1995).

3.1. Computer codes used for the simulation

The computer codes FEN1 and FEN2 have been derived from the computer code FEM301 (Király, 1988), previously developed at the Centre of Hydrogeology of Neuchâtel and submitted to severe and several verification tests under the international HYDROCOIN project (see for example, OECD, 1988).

FEN1 and FEN2 simulate steady state or transient, 1-D, 2-D or 3-D saturated groundwater flow by the finite element method. The programs allow for the incorporation of 1-D, 2-D or 3-D linear or quadratic elements within a 3-D network and are particularly well suited for analysing regional groundwater flow systems in heterogeneous geologic media (e.g. fractured or karst aquifers).

The saturated, constant density, transient groundwater flow is represented by Eq. (6) (Bear, 1979; de Marsily, 1986):

$$S_s \frac{\partial h}{\partial t} + \mathrm{div}(-[K]\cdot \overrightarrow{\mathrm{grad}}\, h) + Q = 0 \tag{6}$$

where S_s is the specific storage coefficient (m^{-1}), $[K]$ is the hydraulic conductivity tensor ($m\ s^{-1}$), h is the hydraulic head (m) and Q represents the general source/sink term (infiltration, well discharge, etc.).

The finite element formulation of the governing partial differential equations is done by the Galerkin method, yielding a set of linear equations. Assembly and solution of the system of linear equations is based on the frontal elimination technique of Irons (1970), which is a particularly useful modification of the Gauss elimination procedure. The frontal method is efficient for large 3-D problems and allows the modeller to rapidly introduce changes in the geometry of the model. The original code FEM301 and the frontal method are described in detail by Király (1985). The time-dependent problem is solved in FEN2 by using the robust Crank–Nicholson implicit time-stepping scheme.

In the present paper, the high hydraulic conductivity channel network is simulated by 1-D quadratic elements, which are located between 2-D or 3-D quadratic elements representing the low hydraulic conductivity fractured limestone volume (see Fig. 1A and 1B).

3.2. Brief description of the simulated configurations

In this paper we present only preliminary results obtained using a number of simplified, 2-D and theoretical karst aquifers. The modelled regions are simple rectangular areas (from 12 to 48 km^2), subdivided into low hydraulic conductivity volumes (K_{low}: $10^{-6}\ m\ s^{-1}$) and high hydraulic conductivity karst channel networks (K_{high}: $50\ m\ s^{-1}$) with various configurations (see Fig. 1A, Fig. 2A, Fig. 3A). The thickness of the aquifer

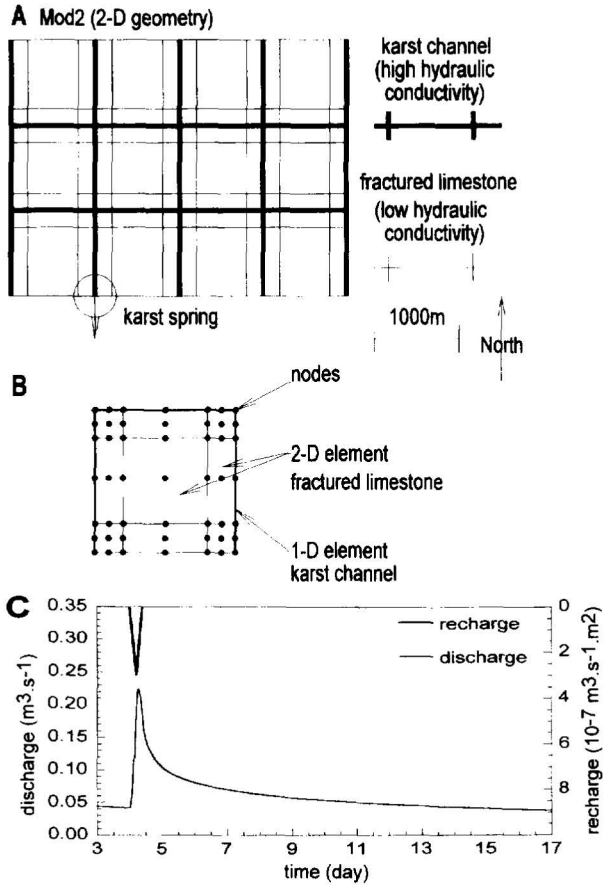

Fig. 2. A: Element network for the variant Mod2. The thin lines represent the boundary of quadratic finite elements. B: Discretization of a fractured limestone volume. C: Global response of Mod2 to a triangular recharge function.

is assumed to be about 50 m. Linear Darcy's law was used throughout the models for both the channel network and the low hydraulic conductivity fractured volume.

The different types of imposed recharge function are shown in Fig. 2C and Fig. 3B, and each aquifer discharges at only one karst spring (see Fig. 1A, Fig. 2A and Fig. 3A). It must be emphasized that 90% of the infiltration is distributed over the low conductivity fractured volume as diffuse infiltration, and only about 10% enters directly into the karst channels as concentrated infiltration. The effect of higher proportions of concentrated infiltration on the karst spring hydrographs is discussed by Király et al. (1995).

The simulated spring hydrographs represent the global response of the modelled aquifer for a given geometrical configuration and a given set of hydraulic parameters (infiltration rates, hydraulic conductivities K_{high} and K_{low}, storativities). Examples of the simulated global responses are shown in Fig. 2C and Fig. 3B. They have been analysed by the global methods described above and the results (that is, the interpretations generally accepted by

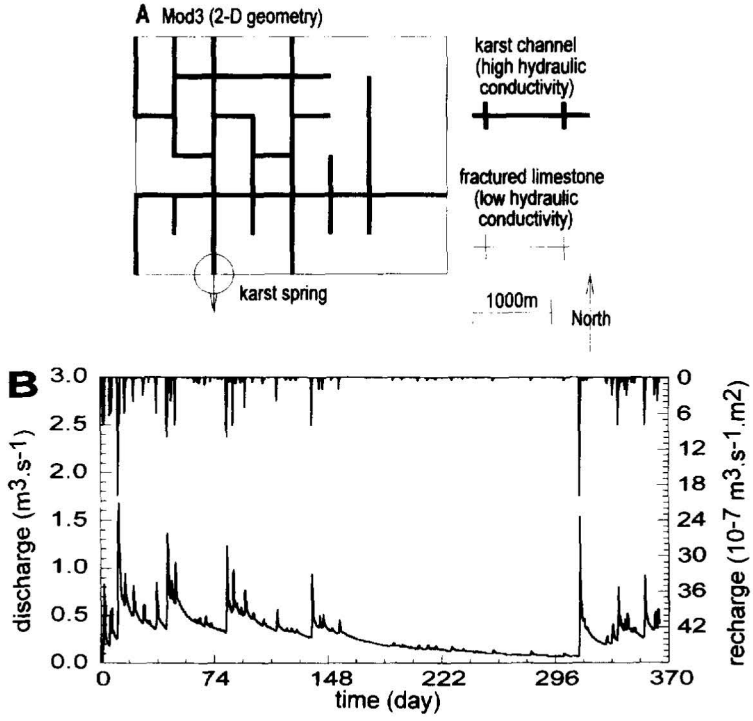

Fig. 3. A: Geometry of the karst channels for variant Mod3. The thin lines represent the boundary of quadratic finite elements. B: Global response of Mod3 to a yearly recharge function.

the users of these methods) are compared to the parameter fields actually introduced into the finite element models.

4. Discussion of the results

We introduced well-defined karst structures into a finite element model and simulated various karst hydrographs. We then analysed the simulated spring hydrographs using the widely accepted global methods. Interpretations from the global methods may lead to erroneous conclusions about the infiltration and groundwater flow processes in karst aquifers (Király and Morel, 1976; Eisenlohr, 1995). The critical remarks hereafter show some of the weak points of the interpretation schemes based on the global methods.

(1) If the recession hydrograph is separated into three or more exponential functions, the intermediate exponentials do not necessarily correspond to the depletion of aquifer volumes with intermediate hydraulic conductivity values. Fig. 4 shows, for example, the simulated recession hydrograph for the variant Mod2. It may be separated into three exponentials, even though we used only two hydraulic conductivities and storativities in the model: one for the high permeablity 1-D elements and another for the low hydraulic conductivity 2-D elements. There is no aquifer volume with an intermediate hydraulic

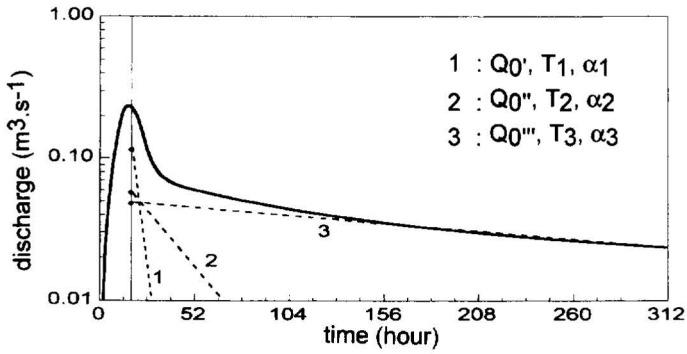

Fig. 4. Separation of a simulated recession hydrograph into three exponential components. The geometry of the aquifer is represented in Fig. 2A, the input function (of triangular type) is shown in Fig. 2C, and the global response is represented in Fig. 2C. $Q0' = 0.12\ m^3\ s^{-1}$; $Q0'' = 0.06\ m^3\ s^{-1}$; $Q0''' = 0.049\ m^3\ s^{-1}$; $a_1 = 0.23\ day^{-1}$; $a_2 = 0.035\ day^{-1}$; and $a_3 = 0.0025\ day^{-1}$.

conductivity, the depletion of which causes the appearance of the intermediate exponential. The intermediate exponential could simply be the result of transient phenomena in the vicinity of the high hydraulic conductivity channel network, as proposed by Király and Morel (1976).

(2) The models show that the baseflow represents the depletion of the low hydraulic conductivity fractured volumes, exactly as assumed in the generally accepted interpretation. It is, however, not true that the recession coefficient α_1 of the baseflow depends on the hydraulic properties of only the low hydraulic conductivity volumes. In fact, it depends greatly on the area and form of the whole aquifer, as well as on the geometry, the hydraulic conductivity and the density of the high hydraulic conductivity channel network. It is a global parameter and will depend on the global configuration of the karst aquifers.

(3) According to traditional interpretation, the non-exponential part of the recession hydrograph would give direct information about the infiltration process. It is assumed, for example, that the time interval between $t = 0$ and $t = 1/\eta$ represents the duration of infiltration (see Eq. (2)). This implies that for $t > 1/\eta$ the infiltration and the non-exponential component of the recession hydrograph will be zero. The simulated hydrographs indicate that these assumptions are not always true. The recession hydrograph represented in Fig. 4, for example, was generated by a recharge event of 24 h. The recharge began at $t =$ 0 h and was stopped after 24 h, $t = 13$ h being the time when the peak discharge occurred. It clearly appears, however, that the non-exponential part of the recession hydrograph extends from $t = 13$ h to about $t = 150$ h. In fact, the duration of the non-exponential part of the recession hydrograph depends on the configuration of the hydraulic parameter fields, the form of the recharge function (Eisenlohr, 1995) and the transient exchange phenomena between the karst channels and the low conductivity fractured volumes. Three-dimensional model results obtained by Király et al. (1995) suggest that even the first part of the baseflow hydrograph might be a non-exponential function.

(4) Correlograms are constructed mainly for long-term hydrographs (several months or years). The indirect verification of their interpretation, involving the use of 3-D aquifer models, is presently under study and results will be presented in a separate paper. As an

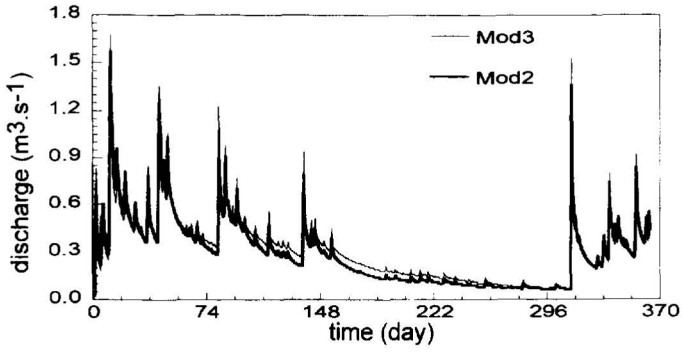

Fig. 5. Hydrographs of 365 days, simulated with the geometry of Mod2 (see Fig. 2A) and Mod3 (see Fig. 3A). The yearly recharge function is shown in Fig. 3B.

example, Fig. 5 shows the global responses of the two aquifers represented in Fig. 2A (Mod2) and Fig. 3A (Mod3) for the recharge function shown in Fig. 3B. The corresponding correlograms are represented in Fig. 6, which also shows the correlogram of the recharge function. The contrast between the aquifers is not enough to generate important differences between the hydrographs. The more slowly decreasing correlogram of Mod3 seems quite normal, as the aquifer is less well drained than in Mod2.

5. Conclusions

Numerical finite element models, even if applied to theoretical and highly simplified karst aquifers, represent an efficient tool for the checking of certain interpretations based on global methods.

The introduction of well-defined karst structures into the finite element models, and the analysis of the simulated karst spring hydrographs by the widely used global methods, indicate that some of the interpretations from the global methods may lead to erroneous conclusions.

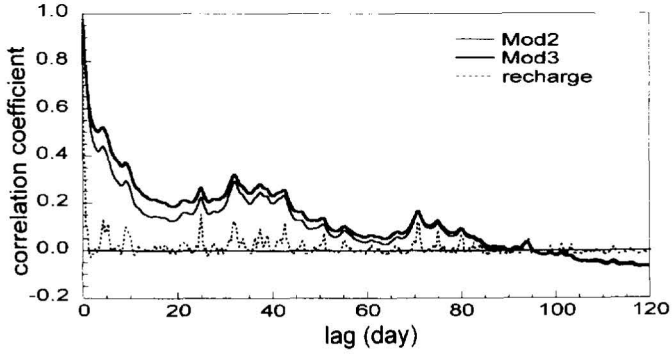

Fig. 6. Simple correlograms for the two hydrographs of Fig. 5 and for the recharge function of Fig. 3B.

In spite of the limitations inherent in the 2-D models, the simulations show clearly that if the karst spring hydrograph is separated into several exponential functions, the exponentials do not necessarily correspond to aquifer volumes with different hydraulic conductivities. The recession coefficient of the last, nearly exponential part of the recession hydrograph depends on the global configuration of the whole karst aquifer, not only on the hydraulic properties of the low hydraulic conductivity volume.

References

Atkinson, T.C., 1977. Diffuse flow and conduit flow in limestone terrain in the Mendip Hills, Somerset (Great Britain). J. Hydrol., 35: 93–103.

Bear, J., 1979. Hydraulics of Groundwater. McGraw-Hill, London, 569 pp.

Bonacci, O., 1987. Karst Hydrology. Springer-Verlag, Berlin, 173 pp.

Bonacci, O., 1993. Karst springs hydrographs as indicators of karst aquifers. J. Hydrol. Sciences, 38(1–2): 51–62.

Box, G.E.P. and Jenkins, G.M., 1974. Time Series Analysis: Forecasting and Control. Holden-Day, San Francisco, 575 pp.

Dreiss, S.J., 1982. Linear kernels for karst aquifers. Water Resour. Res., 18(4): 865–876.

Drogue, C., 1972. Analyse statistique des hydrogrammes de décrues des sources karstiques. J. Hydrol., 15: 49–68.

Eisenlohr, L., 1995. Variabilité des réponses naturelles des aquifères karstiques. De l'identification de la réponse globale vers la connaissance de la structure de l'aquifère. Thèse Doc. ès Sci., Université de Neuchâtel, Centre d'Hydrogéologie, Switzerland.

Forkasiewicz, J. and Paloc, H., 1967. Le régime de tarissement de la Foux de la Vis. Etude préliminaire. AIHS Coll. Hydrol. des roches fissurées, Dubrovnik (Yugoslavia), Vol. 1, pp. 213–228.

Irons, B.M., 1970. A frontal solution program for finite element analysis. Int. J. Num. Math. Eng., 2: 5–32.

Király, L., 1975. Rapport sur l'état actuel des connaissances dans le domaine des caractères physiques des roches karstiques. In: Hydrogeology of Karstic Terrains (eds. Burger et Dubertret), Union of Geological Sciences, Series B, Vol. 3, pp. 53–67.

Király, L. and Morel, G., 1976. Remarques sur l'hydrogramme des sources karstiques simulées par modèles mathématiques. Bull. Centre Hydrogéol., Neuchâtel, 1: 37–60.

Király, L., 1979. Remarques sur la simulation des failles et du réseau karstique par éléments finis dans les modèles d'écoulement. Bull. Centre d'Hydrogéol. Neuchâtel, 3: 155–167.

Király, L., 1985. FEM 301: A three dimensional model for groundwater flow simulation. NAGRA Technical Report 84–49, Baden, Switzerland, 140 pp.

Király, L., 1988. Large scale 3-D groundwater flow modelling in highly heterogeneous geologic medium. In: Groundwater Flow Quality Modelling (eds. Custodio et al.), Reidel Publishing Co., 224, pp. 761–775.

Király, L., Perrochet, P. and Rossier, Y., 1995. Effect of the epikarst on the hydrograph of karst springs: a numerical approach. Bull. Centre d'Hydrogéol. Neuchâtel, 14: 1–22.

Mangin, A., 1975. Contribution à l'étude hydrodynamique des aquifères karstiques. Thèse Doc. ès Sci.; Annales de spéléol., 29: 285–382, 495–601, 30: 21–124.

Mangin, A., 1984. Pour une meilleure connaissance des systèmes hydrologiques à partir des analyses corrélatoire et spectrale. J. Hydrol., 67: 25–43.

de Marsily, G., 1986. Quantitative hydrogeology. In: Groundwater hydrology for engineers, Academic Press, London, 435 pp.

OECD, 1988. The international HYDROCOIN Project. Level 1: code verification. OECD Publications, Paris, 198 pp.

Padilla, A., Pulido-Bosch, A. and Mangin, A., 1994. Relative importance of baseflow and quickflow from hydrographs of karst spring. Ground Water, 32(2): 267–277.

Schoeller, H., 1967. Hydrodynamique dans le karst. Chronique d'Hydrogéol., BRGM, 10: 7–21.

Soulios, G., 1991. Contribution à l'étude des courbes de récession des sources karstiques: Exemples du pays Hellénique. J. Hydrol., 127: 29–42.